UCRL-18390

cy. 2

RECEIVED
LAWRENCE
RADIATION LABORATORY

OCT 21 1968

LIBRARY AND
DOCUMENTS SECTION

University of California

Ernest O. Lawrence Radiation Laboratory

PAIRING EFFECTS AT THE FISSION SADDLE POINT OF ^{210}Po AND ^{211}Po

L. G. Moretto, R. C. Gatti, S. G. Thompson,
J. R. Huizenga, and J. O. Rasmussen

August 1968

TWO-WEEK LOAN COPY

This is a Library Circulating Copy which may be borrowed for two weeks. For a personal retention copy, call Tech. Info. Division, Ext. 5545

Berkeley, California

UCRL-18390 cy. 2

DISCLAIMER

This document was prepared as an account of work sponsored by the United States Government. While this document is believed to contain correct information, neither the United States Government nor any agency thereof, nor the Regents of the University of California, nor any of their employees, makes any warranty, express or implied, or assumes any legal responsibility for the accuracy, completeness, or usefulness of any information, apparatus, product, or process disclosed, or represents that its use would not infringe privately owned rights. Reference herein to any specific commercial product, process, or service by its trade name, trademark, manufacturer, or otherwise, does not necessarily constitute or imply its endorsement, recommendation, or favoring by the United States Government or any agency thereof, or the Regents of the University of California. The views and opinions of authors expressed herein do not necessarily state or reflect those of the United States Government or any agency thereof or the Regents of the University of California.

To be submitted to:
Physical Review

UCRL-18390
Preprint

UNIVERSITY OF CALIFORNIA

Lawrence Radiation Laboratory
Berkeley, California 94720

AEC Contract No. W-7405-eng-48

PAIRING EFFECTS AT THE FISSION SADDLE POINT OF ^{210}Po AND ^{211}Po

L. G. Moretto, R. C. Gatti, S. G. Thompson,
J. R. Huizenga, and J. O. Rasmussen

August 1968

PAIRING EFFECTS AT THE FISSION SADDLE POINT OF ^{210}Po AND ^{211}Po†

L. G. Moretto*, R. C. Gatti, S. G. Thompson

Lawrence Radiation Laboratory, University of California
Berkeley, California 94720

and

J. R. Huizenga

Department of Chemistry and Physics, University of Rochester
Rochester, New York 14627

and

J. O. Rasmussen

Departments of Chemistry and Physics, University of California
Berkeley, California 94720

August 1968

ABSTRACT

The fission-fragment angular distributions were measured for ^{4}He induced fission of ^{206}Pb and ^{207}Pb targets. The compound nuclei ^{210}Po and ^{211}Po were obtained at excitation energies ranging from 3 to 20 MeV above the fission barriers.

The experimental data were fitted by a theoretical expression relating the angular distribution of fission fragments to the distribution of the total angular momentum I and of the angular momentum projection K on the nuclear symmetry axis at the saddle point. By a least squares fitting procedure the variance K_o^2 of the K distribution was obtained.

In the case of the even-even nucleus ^{210}Po the K_o^2 value approaches zero at about 3 MeV above the barrier while in the case of the odd A nucleus ^{211}Po, K_o^2 remains rather large: this indicates the presence of the pairing gap in ^{210}Po and of the residual quasi particle in ^{211}Po.

Furthermore the approximately constant difference in K_o^2 between the even-even and odd-A nucleus at corresponding energies is consistent with the expected contribution of a single quasi particle to K_o^2.

From the analysis of the data, the value of the pairing gap 2Δ at the saddle point of ^{210}Po is estimated to be about 4 MeV, about two to three times larger than in the ground state.

The odd-even differences of saddle point masses are also analyzed and the dependence of pairing on the nuclear surface is discussed.

I. INTRODUCTION

Nuclei in their fission saddle-point configurations exhibit "transition state" spectra which resemble those of deformed nuclei in their stable equilibrium configurations.[1] In general however, the fission saddle point is characterized by much larger deformations than those of the ground state nuclei. Therefore the study of nuclei at the saddle point can provide information about nuclear properties at unusually large deformations. The properties of the transition-state nuclei can be investigated by measurements of fission-fragment angular distributions.

While at very small excitation energies above the barrier the angular distributions can be interpreted in terms of a few transition-state levels, at energies larger than a few MeV only a statistical analysis is possible. Halpern and Strutinski[2] and Griffin[3] have used the assumption of statistical distribution of levels at the saddle point to calculate the angular distributions at medium-low excitation energies and attempted to fit experimental data. The energy dependence was determined in terms of the Fermi gas model. The conclusion of the analysis seems to be that, while the shape of the angular distributions is reproduced very well, the expected dependence on the excitation energy is verified by the experiment no more than qualitatively. The idea that at relatively low excitation energies the Fermi gas model is expected to fail and that the pairing effects must be considered has been expressed by Halpern and Strutinski,[2] Griffin,[4] and Vandenbosch et al.[5]

An attempt to measure the saddle-point pairing effects was made by Griffin[6] who analyzed angular distribution data of Vandenbosch et al.[5] on ^{237}Pu and of Simmons[7] on ^{240}Pu compound nuclei. The gap parameter obtained was Δ_0 = 1.36 MeV

which implied a pairing gap of $2\Delta_0 = 2.72$ MeV for ^{240}Pu. This value is more than twice the value in the ground state. Further experiments by H. Britt et al.[8] using ^{239}Pu (d,pf) reaction succeeded in estimating the value $2\Delta_0 = 2.6^{+0.21}_{-0.45}$ MeV for ^{240}Pu at the saddle point. More recent experiments by Rickey and Britt[10] gave the value $2\Delta_0 = 1.98 \pm 0.15$ MeV for ^{240}Pu and $2\Delta_0 = 2.10 \pm 0.15$ MeV for ^{236}U.

The rather large value of the pairing effects at the saddle point was observed much earlier by Swiatecki[11] in his investigation of the even-odd mass differences at the saddle point of nuclei heavier than thorium. He observed that while the odd-odd, odd, and even-even families of nuclear masses in the ground state are separated by about 0.77 mMU, at the saddle point the same families are separated by about 1.2 mMU. Fong[12] also discusses the same effect. This increase in pairing effects in the transition-state spectrum was attributed[13] to the increase in surface area of the nucleus at the saddle point. Some calculations by Kennedy et al.[13] on the slab model of a nucleus show that while infinite nuclear matter presented vanishingly small pairing effects, the slab model calculations predicted a finite pairing gap very sensitive to the slab thickness.

To shed more light on the problem we attempted to determine the pairing effects at the saddle points of ^{210}Po and ^{211}Po. The reason for this choice is twofold: (a) The increase in surface area at the saddle point is for these nuclei ~20% according to liquid-drop calculations[14] while for ^{240}Pu it is 10% relative to the spherical shape and less when one considers the deformation already present in the ground state; (b) The fission probability near the barrier, though very low, is still sufficient to allow the measurement of fission-fragment angular distributions. The reason for the choice of the even-odd pair was the expectation that systematic even-odd differences in the properties of the transition spectrum could be observed.

II. THEORETICAL EXPRESSION FOR THE ANGULAR DISTRIBUTION

An axially symmetric nucleus at the fission saddle point is characterized by three angular momentum quantum numbers which are the total angular momentum I, the projection of I on the space-fixed z axis M, and the projection of I on the body-fixed symmetry axis K. If K stays constant from the saddle point to infinity, the probability distribution of the symmetrical top wave function at the saddle point determines the fission-fragment angular distribution. The constancy of K is classically dependent on the preservation of axial symmetry from saddle to infinity; this assumption is partially supported by the liquid-drop model which predicts axially symmetric saddle-point shapes, and by the pairing effects which tend to preserve axial symmetry. Furthermore, the stage between saddle and scission point seems to be so short[14] that the Coriolis interaction might be prevented from effectively mixing levels with different K. If some limited K mixing from Coriolis or γ-vibrational interactions is present, the theoretical approach may still be valid. A strong evidence of the goodness of the K quantum number comes from the sharpness of the experimental angular distributions themselves. Assuming then that K is a good quantum number, the angular distribution of fission fragments from a system characterized by a given set of I, M, K values will be:

$$W^{I}_{M,K}(\theta) = \frac{2I+1}{4\pi}\left|D^{I}_{M,K}(\phi,\theta,\chi)\right|^{2} , \qquad (1)$$

where $D^{I}_{M,K}$ is the symmetrical-top wave function and ϕ, θ, and χ are the Eulerian angles that define the position of the body with respect to the rest frame of reference.

Since the quantity $D^{I}_{M,K}$ can be written explicitly as

$$D^{I}_{M,K}(\phi,\theta,\chi) = d(\theta)\, e^{iM\phi}\, e^{iK\chi} , \qquad (2)$$

it follows that $\left|D^I_{M,K}\right|^2$ is a function only of the angle θ between the space-fixed and body-fixed axis.

For large I the angular distribution can be expressed in the following approximate form:[15]

$$W^I_{M,K}(\theta) = \frac{2I+1}{4\pi^2}\left[(I+1/2)^2\sin^2\theta - M^2 - K^2 + 2MK\cos\theta\right]^{-1/2} \tag{3}$$

In order to reproduce the angular distributions of fission fragments obtained in particle bombardments, the above expression must be averaged over the K and I distributions.

Following Halpern and Strutinski[2] we assume the K distribution to be of the form: $\exp(-K^2/2K_o^2)$. If M = 0, for fixed I and K_o^2 the angular distribution will be:

$$W^I_{K_o^2}(\theta) = \frac{2I+1}{4\pi^2}\,\frac{\int_0^{(I+1/2)\sin\theta} dK\left[(I+1/2)^2\sin^2\theta - K^2\right]^{-1/2}\exp(-K^2/2K_o^2)}{\int_0^{I+1/2} dK\,\exp(-K^2/2K_o^2)} \tag{4}$$

The upper limit of the integral in the numerator represents the highest value of K which is classically possible at every angle θ. By executing the integration we have:

$$W^I_{K_o^2}(\theta) = \left(\frac{2}{\pi}\right)^{1/2}\frac{1}{4\pi}\frac{(2I+1)}{2\sqrt{K_o^2}}\left(\mathrm{erf}\,\frac{I+1/2}{\sqrt{2K_o^2}}\right)^{-1}\exp\left(-\frac{(I+1/2)^2\sin^2\theta}{4K_o^2}\right)J_o\left(i\,\frac{(I+1/2)^2\sin^2\theta}{4K_o^2}\right) \tag{5}$$

where erf is the error function and J_o is the Bessel function of order zero.

The angular momentum distribution for the compound nucleus can be obtained by analyzing the reaction mechanism involved in its formation. In the present case, involving a particle bombardment with compound nucleus formation, the total angular momentum distribution can be obtained from an optical model calculation.

If we assume that the nuclei at the saddle point have the same I distribution as the compound nucleus, the final angular distribution averaged over K and I will then be:

$$W(\theta) \propto \sum_{I=0}^{\infty} (2I+1)^2 \, T_I \left(\mathrm{erf} \frac{I+1/2}{\sqrt{2K_o^2}} \right)^{-1} \exp\left(- \frac{(I+1/2)^2 \sin^2\theta}{4 \, K_o^{\,2}} \right) J_o\left(i \, \frac{(I+1/2)^2 \sin^2\theta}{4 \, K_o^{\,2}} \right) \quad (6)$$

where T_I are the optical-model transmission coefficients. This approximate expression has been shown to be very satisfactory when compared with the expression obtained using the symmetrical-top wave functions in their exact quantum mechanical form.[16]

III. EXPERIMENTAL PROCEDURE

The experiments were designed to measure the fission-fragment angular distributions of He^4 induced fission of Pb^{206} and Pb^{207}. The lowest excitation energy for which angular distributions were measured was about 3 MeV above the fission barrier. The highest excitation energy, about 20 MeV above the barrier, was determined on the basis of substantial onset of multiple-chance fission as estimated from the cross section data.

Mica was used for detecting the fission fragments[17] because of its good performance and convenience when very small cross sections are involved, as was the case here. The experimental setup consisted of a small fission chamber as indicated in Fig. 1, in which a mica holder was fitted. The mica strip was laid on a cylindrical surface whose radius was 2.84 cm. The exposed surface of mica ranged in angle from 45° to 205° with respect to the beam direction. At 205° a shield was used to cover the mica and give a sharp cutoff in the fission-fragment distribution, which served as an angular reference point. The height of the exposed part of the mica strip was 1 cm.

Particular care was taken in preparing high purity targets because of the very low cross sections ($< 10^{-32} cm^2$) at the lowest excitation energies above the barrier. With such cross sections even one part in 10^9 of uranium or thorium would contribute enough fission events to cause a substantial error in the experiment. The target backing consisted of a water-cooled copper block that was fitted in the center of the chamber at an angle of 45° with respect to the beam direction. The surface on which the target material was to be deposited was first covered with a thickness of more than 20 mg/cm^2 of high purity silver deposited by evaporation. This layer prevented fission fragments coming from the impurities in the copper

from escaping and entering the mica. The target materials, monoisotopic ^{206}Pb and ^{207}Pb in the form of metal, were evaporated on the silver. In preparing the targets by vaporization of the lead isotopes, early and late fractions of the distillate were excluded since they are most likely to contain the highest levels of impurities. It is especially desirable to avoid collecting the late fractions because the uranium and thorium impurities tend to concentrate there. The purity of the targets was checked by two methods. The first involved bombarding at energies below the fission barriers of ^{210}Po and ^{211}Po and searching for fission events which might come from impurities with lower fission barriers such as uranium or thorium. The second method consisted in checking the steepness of the cross-section curves as a function of energy at energies near the barrier.

The thickness of the targets ranged between 1 and 3 mg/cm^2. The effects of the thickness of the target on the angular distributions were determined experimentally and found to be negligible up to 3 mg/cm^2 thickness for angles between 85° and 175°. The position of the beam on the target was determined by a collimator 22.35 mm long and 1.59 mm in diameter and by the low convergence of the beam, controlled by a quadrupole focussing lens 7 meters away from the collimator. The beam current was read from the target itself without a separate Faraday cup.

The variable energy beam of the ^{4}He particles was provided by the 88 in. variable-frequency cyclotron in Berkeley. The mica strips obtained from the experiment were etched with hydrofluoric acid (48%) for 5 to 6 hours. In this way the diamond-shaped fission tracks were observed using an optical microscope (Fig. 2) with a total magnification ranging from 60× to 200×.

Rectangular strips of the mica were scanned almost continuously over angles ranging from 85° to 172°. The angular correction for the aberration introduced by the scanning technique is presented in the Appendix. The angular width of the strips was 3° or smaller since the angular resolution of the system was about 3°.

IV. ANALYSIS OF THE DATA

The experimental angular distribution data were first transformed to the center-of-mass system. In this case the assumption was made that all of the fission fragments had the same kinetic energy equal to half the average total kinetic energy. The total kinetic energy for ^{210}Po was taken as 146.6 MeV and for ^{211}Po as 146 MeV (see the experimental data of R. Vandenbosch and J. R. Huizenga.[18]) The dispersion in angle introduced by the variations in kinetic energy of fission fragments and by the neutrons evaporating from the fragments was estimated to be of the order of 1°. The center-of-mass angular distributions were fitted with Eq. (6). The fitting parameters were the value of a normalization constant and the quantity K_o^2.

The coefficients T_I were obtained from an optical model calculation on the $^{206}Pb + {}^4He$ and $^{207}Pb + {}^4He$ reactions using a Wood-Saxon potential. The parameters used were:

^{206}Pb	^{207}Pb
$V = -50$ MeV	$V = -50$ MeV
$W = -23.00$ MeV	$W = -23.12$ MeV
$r_o = 1.17\ A^{1/3}$ fm	$r_o = 1.17\ A^{1/3}$ fm
$r_\alpha = 1.77$ fm	$r_\alpha = 1.77$ fm
$d = 0.576$ fm	$d = 0.576$ fm

These parameters have been taken or extrapolated from the work of Huizenga and Igo.[19]

The effect of the ^{207}Pb target spin 1/2 on the angular distribution has been neglected. An estimate of such an effect has been done following J. Griffin.[20] The change in the predicted anisotropy has been evaluated and found to be smaller than 1.5%.

Some examples of experimental angular distributions, together with the theoretical fits are shown in Figs. 3, 4, 5, 6. The values of K_o^2 versus E obtained from the data fitting are presented in Figs. 7, 8 and Tables I and II. The quoted errors are calculated from the statistical errors of the experimental data. No other random error has been estimated. The expression for the angular distributions has been found to be very satisfactory in fitting all of the experimental data. The center-of-mass anisotropy W(180°)/W(90°) obtained from the best fit curves and the average of the square of angular momentum $\langle \ell^2 \rangle$ obtained from the optical model calculations are also given in Tables I and II.

V. DISCUSSION

In order to estimate the magnitude of the pairing effects at the saddle point, a knowledge of the fission barriers of the nuclei being considered is essential. The best estimate available at present for the ^{210}Po fission barrier has been obtained by Thompson et al.[21] In their experiments the fission cross sections for the reactions ^{206}Pb + ^{4}He and ^{209}Bi + ^{1}H were measured over a large range of energies going down to cross sections as low as 10^{-35} cm^{2}. Theoretical expressions derived by Huizenga et al.[22] and by Burnett et al.[23] were used to fit the data expressed in the form of the ratio Γ_f/Γ_n. The fission barriers deduced from fitting the data when the parameters were varied over rather large reasonable ranges averaged 19.82 MeV for ^{209}Bi + ^{1}H and 20.25 for ^{206}Pb + ^{4}He. These calculations do not include pairing effects. Thus for even-even compound nuclei the level density at the saddle point will tend to make the above values overestimates so that the real barriers should be somewhat lower. Nonetheless we shall take 20 MeV as the nominal value for ^{210}Po with the mental reservation that the true value could be somewhat lower. This uncertainty means only that the value of the gap estimated in the present work is a lower limit, and the magnitude of the gap could be even larger.

In the case of ^{211}Po no measured barrier is available. We then rely on two ways of making an estimate: (1) from Myers and Swiatecki's mass formula[24] the fission barrier is calculated to be 20 MeV (note that the saddle masses have been normalized to the ^{201}Tl experimental value[23]). (2) From Thompson et al.[21] we have taken the measured fission barriers of the following odd nuclei: ^{201}Tl, ^{207}Bi, ^{209}Bi, and ^{213}At and subtracted from them the mass shift due to the shell effect in the ground state. We have plotted these corrected values as a function of the fissility parameter x. By interpolation and correction for the shell effect

we obtained for the ^{211}Po barrier about 19.8 MeV, very close to the Myers-Swiatecki predicted value.

Once the barrier height is known, we can make a comparison with the predictions of the Fermi gas model. This model relates K_o^2 to the excitation energy E_s^x over the saddle point as follows:[2]

$$K_o^2 = \frac{\mathfrak{I}_{eff}}{\hbar^2} T \quad . \tag{7}$$

T is the nuclear temperature at the saddle point which is related to the excitation energy at the saddle point E_s^x by the expression:

$$T^2 = E_s^x / a_f \quad , \tag{8}$$

a_f being the level density parameter at the saddle point. The effective moment of inertia $\mathfrak{I}_{eff}$ is related to the moment of inertia about the symmetry axis $\mathfrak{I}_{\parallel}$ and about an axis perpendicular to it $\mathfrak{I}_{\perp}$ by the expression

$$\mathfrak{I}_{eff}^{-1} = \mathfrak{I}_{\parallel}^{-1} - \mathfrak{I}_{\perp}^{-1} \quad . \tag{9}$$

The values of K_o^2 obtained from both the experimental data and from Eq. (7) are shown in Fig. 9. The value of $\mathfrak{I}_{eff}$ was taken from the liquid drop calculations of Cohen and Swiatecki,[25] and a_f was taken equal to A/8.[20] This curve does not represent an actual fitting to the data. It merely indicates the disagreement between theoretical predictions and experimental data. The fact that K_o^2 is lower than predicted on the basis of the Fermi gas assumption can be accounted for in terms of pairing effects. In particular we observe that in the ^{210}Po case, K_o^2 drops rapidly to zero at about 3 MeV above the saddle point. More precisely, at 3 MeV above the "nominal" barrier, $K_o^2 = 3.3$. This value is so small that it can be explained in terms of collective excitation states (rotational and vibrational) within the gap, precluding any substantial contribution by intrinsic

(two quasi particle) excitations. Also the next higher point has a value $K_o^2 = 8.8$ that could be explained both by collective excitations and intrinsic excitations. This indicates that the pairing gap for ^{210}Po at the saddle point is at least 3 MeV. An immediate check in the ^{211}Po case shows that K_o^2 does not drop to zero even at 3 MeV above the barrier. This is to be expected for an odd nucleus for which a gap is absent because the odd particle provides intrinsic excitations at all energies.

Another large effect that can be observed is the overall difference between the two K_o^2 curves. The ^{211}Po curve follows the trend of the ^{210}Po curve rather well, but lies higher by about 7.5 units of K_o^2. If this is an even-odd effect, then we can conclude that the average contribution of one quasi particle to K_o^2 is about 7.5 units. This checks rather well with a calculation based on the Nilsson model. We have calculated the average square of the Ω values of the Nilsson orbitals about the Fermi level. At the maximum deformation available in Nilsson calculations[27] ($\epsilon = 0.6$), $\overline{\Omega^2}$ is about 8 for neutrons and 5 for protons (average over 16 levels) giving an overall average of 6.5. With this contribution to K_o^2 of one quasi particle, one can check whether some of the structure visible in the plots of K_o^2 for ^{210}Po and ^{211}Po are related to the onset of different numbers of quasi particles. In ^{210}Po two flattenings occur at $K_o^2 \cong 16$ and $K_o^2 \cong 29$, values close to twice and four times the contributions of 7.5 units found for one quasi particle. In ^{211}Po two flattenings occur at $K_o^2 \cong 22.5$ and $K_o^2 \cong 37.5$, values again very close to three and five times the one-quasi particle contribution. The very definite possibility of different values for the gap parameter for neutrons and protons makes it difficult to decide the quantitative significance of the above structure. However, their positions in excitation energy, as well as the absolute values of K_o^2 as a function of energy, when compared

with the one-quasi particle contributions, still suggest a rather larger value for the pairing gap than the lower limit previously discussed, possibly 4 MeV or larger.

Gap Parameter from Even-Odd Mass Differences at the Saddle Point

The difference in fission barriers between odd-A and even-even isotopes can provide in principle some information about the gap parameters Δ_s at the saddle point, just as the ground state even-odd mass differences allow the evaluation of the ground state gap parameter Δ_g. It is therefore of interest to analyze this problem since we have reasonably good values for the fission barriers of ^{210}Po and ^{211}Po.

Let us assume with Myers and Swiatecki[24] and Strutinski[28] that shell and pairing effects are separable from a smooth liquid-drop-like term. This term can be derived from a pure single particle model with smoothly varying level spacing and including surface, symmetry, coulomb energy and any other term which is of single particle and electromagnetic nature. Using such a single particle model for the energy base-line, we can express the fission barrier of an even-even nucleus, B_f^e as follows (see Fig. 10):

$$B_f^e = B_{sp}^e + \text{Shell}_g^e + C_g^e - \text{Shell}_s^e - C_s^e \qquad (10)$$

where B_{sp}^e is the term deriving from the single particle (liquid drop-like) model.

Shell_g^e and Shell_s^e are the shell terms in the ground state and saddle point respectively, due to the bunching of single particle levels.

C_g^e and C_s^e are the condensation energies due to pairing in the ground state and saddle point respectively.

In order to obtain the fission barrier for an odd-A nucleus, we must add the lowest one-quasi-particle excitation to both the paired ground state and

saddle point of the corresponding even-even nucleus; we can also make allowance for smooth changes due to the introduction of the extra particle. The one-quasi-particle excitation energy is

$$E = \sqrt{(\epsilon - \lambda)^2 + \Delta^2} \approx \Delta$$

where λ is the Fermi level and ϵ is the energy of the single particle level closest to it. Then the fission barrier, B_f^o, for an odd-A nucleus can be written (see Fig. 10):

$$B_f^o = B_{sp}^o + \text{Shell}_g^o + C_g^o - \Delta_g - \text{Shell}_s^o - C_s^o + \Delta_s \qquad (11)$$

where Δ_g and Δ_s are the gap parameters at the ground and saddle point respectively and the other terms are the equivalent to those described in the previous expression.

From (10) and (11) we obtain:

$$\Delta_s - \Delta_g = (B_f^o - B_f^e) - (B_{sp}^o - B_{sp}^e) - (\text{Shell}_g^o - \text{Shell}_g^e) + (\text{Shell}_s^o - \text{Shell}_s^e) - (C_g^o - C_g^e) + (C_s^o - C_s^e) \qquad (12)$$

The two terms $(C_g^o - C_g^e)$ and $(C_s^o - C_s^e)$ should be small because the main effect of the odd particle is included in the one-quasi-particle excitation and should be of negative sign because of the blocking effect of the odd particle. Since the two terms appear with opposite sign, one might disregard them for lack of better knowledge.

The term $(\text{Shell}_s^o - \text{Shell}_s^e)$ is likely to be small for large saddle deformations. Instead, the term $(\text{Shell}_g^o - \text{Shell}_g^e)$ is dependent on the position of the two nuclei with respect to a closed shell and can be as large as a few MeV; therefore it cannot be disregarded.

The term $(B_{sp}^o - B_{sp}^e)$ can be evaluated from liquid drop calculations and its magnitude is of the order of a few tenths of one MeV if the odd particle is a

neutron and of the order of one MeV if the odd particle is a proton.

The relation

$$\Delta_s - \Delta_g = B_f^o - B_f^e \tag{13}$$

has been used by Griffin[6] and by Stepien and Szymanski.[29] It seems from the above considerations that such an expression could be very unreliable in obtaining the saddle point gap parameter Δ_s.

We can now apply Eq. 12 to the ^{210}Po, ^{211}Po pair to estimate the gap parameter Δ_s at the saddle point. If we take the fission barrier values previously discussed and the shell effects and liquid-drop terms from Myers and Swiatecki,[24] we obtain $\Delta_s - \Delta_g = 1.0$ MeV; it is difficult to establish the uncertainties of this quantity, but, on the basis of the discussion of the ^{210}Po fission barrier in Section 4, it could be somewhat larger. Using for Δ_g the value of 0.81 MeV given by P. E. Nemirovsky and Yu. V. Adamchuk[30] (this value, obtained from even-odd mass differences, has been corrected for shell effects and other liquid-drop contributions), we obtain $\Delta_s = 1.81$ MeV and then the pairing gap $2\,\Delta_s = 3.62$ MeV, in agreement with the value obtained from the angular distribution analysis.

Possible Reasons for the Large Pairing Effects

There is no satisfactory explanation as yet for the very large pairing effects observed at the saddle point. However, it is interesting to consider some possible causes of such effects.

From the uniform model, the gap parameter Δ can be expressed approximately in terms of the density g of Nilsson levels near the Fermi level and pairing strength G as follows:

$$\Delta = S\, e^{-1/gG}, \tag{14}$$

where S is the energy interval above and below the Fermi surface over which the pairing interaction extends.

An accidental bunching of levels about the Fermi surface at the saddle point deformation could in principle result in an increase in g sufficient to explain the observed effect. However such an explanation may be ruled out if the experimental results continue to show more cases in which a larger value of Δ is observed at the saddle point than in the ground state, especially if the observations are made over a large range of deformation. Even the present data together with the data available for ^{236}U and ^{240}Pu tend to rule out the hypothesis that the effect is due only to the accidental bunching of levels. An increase of pairing strength G with an increase in the surface of the nucleus resulting from deformation is considered to be a more likely explanation.

The dependence of the gap parameter Δ on the nuclear surface has been studied by Kennedy et al.[13] They observed that infinite nuclear matter calculations with realistic nucleon-nucleon potentials yielded very low values for the pairing gap. The physical reason for this effect can be understood as follows: the Fermi momentum for the nuclear matter density corresponds to collision energies of about

80 MeV in the center-of-mass between two nucleons. At this energy the repulsive core in the nucleon-nucleon potential approximately compensates for the attractive part of the potential. On the other hand a calculation carried out for a slab of nuclear matter of finite thickness and infinite extension yielded a substantial pairing gap whose magnitude was very sensitive to the slab thickness. This can be understood by noticing the lower density in the surface region. The lower density implies a lower Fermi momentum, for which the hard core of the nucleon-nucleon potential is not strongly felt.

Stepien and Szymanski[29] attempted to explain the large pairing gap at the saddle point by assuming that the pairing strength increases proportionally to the nuclear surface as the nucleus deforms from the equilibrium configuration to the saddle point. They also quote some results of gap parameter calculations carried on in the rare earths region. In these calculations the BCS equations were solved for increasing values of the pairing strength. By making the same assumptions we can obtain a general approximate relation between Δ and s.

We write:

$$G = G_o \left(1 + \frac{\delta s}{s}\right) \quad , \tag{15}$$

where $\frac{\Delta s}{s}$ is the fractional surface increase; substituting in (14) we obtain

$$\ln \frac{\Delta}{\Delta_o} = \frac{1}{gG_o} \left[\frac{\frac{\delta s}{s}}{1 + \frac{\delta s}{s}} \right] \tag{16}$$

The quantity gG_o is dimensionless and has a value of about 1/3. The increase in Δ as a function of $\frac{\delta s}{s}$ is presented in Fig. 11. The agreement between this general calculation and the specific case reported by Stepien and Szymanski is good, but it appears that the increase in gap predicted in this way is not quite large enough to reproduce the experimental data.

ACKNOWLEDGMENTS

We would like to thank J. R. Nix, W. J. Swiatecki and S. G. Nilsson for their helpful discussions and suggestions. We are indebted to N. Glendenning for the use of his optical model program.

We are very grateful to Mrs. Claudette Rugge for the development of the program to fit the angular distribution data.

FOOTNOTES AND REFERENCES

†Work performed under the auspices of the U. S. Atomic Energy Commission.

*On leave from University of Pavia, Pavia, Italy.

1. A. Bohr, Proceedings of the First United Nations International Conference on the Peaceful Uses of Atomic Energy (United Nations, New York, 1956), Vol. 2, p. 151, Paper P/911.
2. I. Halpern and V. M. Strutinski, Proceedings of the Second United Nations International Conference on the Peaceful Uses of Atomic Energy (United Nations, Geneva, 1958), Vol. 15, p. 408, Paper P/1513.
3. J. J. Griffin, Phys. Rev. 116, 107 (1959).
4. J. J. Griffin, Proceedings of the International Conference on Nuclear Structure, Kingston, Canada, 1960 (University of Toronto Press, Toronto, 1960) p. 843.
5. R. Vandenbosch, H. Warhanek, and J. R. Huizenga, Phys. Rev. 124, 846 (1961).
6. J. J. Griffin, Phys. Rev. 132, 2204 (1963).
7. J. E. Simmons, R. B. Perkins, and R. L. Henkel, Phys. Rev. 137, B809 (1966).
8. H. Britt, R. Stokes, W. Gibbs, and J. J. Griffin, Phys. Rev. Letters 11, 343 (1963).
9. H. Britt, R. Stokes, W. Gibbs, and J. J. Griffin, Phys. Rev. 139, B345 (1965).
10. F. A. Rickey, Jr. and H. C. Britt, Bull. Am. Phys. Soc. 13, 36 (1968).
11. W. Swiatecki, Phys. Rev. 100, 936 (1955).
12. P. Fong, Phys. Rev. 122, 1545 (1961).
13. R. C. Kennedy, L. Wilets, and E. M. Henley, Phys. Rev. Letters 12, 36 (1964).
14. James Rayford Nix, Further Studies in the Liquid-Drop Theory of Nuclear Fission (UCRL-17958, July 1968), to be submitted to Nucl. Phys.

15. T. A. Wheeler, Fast Neutron Physics, Part II, J. B. Marion and J. L. Fowler, eds., (Wiley and Sons, Interscience, New York, 1963).

16. J. R. Huizenga, A. N. Behkami, and L. G. Moretto, Note on Interpretation of Fission-Fragment Angular Distributions at Moderate Excitation Energies, to be submitted to Phys. Rev.

17. P. B. Price and R. M. Walker, J. Appl. Phys. 33, 2625, 3407 (1962).

18. R. Vandenbosch and J. R. Huizenga, Phys. Rev. 127, 212 (1962).

19. J. R. Huizenga and G. Igo, Nucl. Phys. 29, 462 (1962).

20. J. J. Griffin, Phys. Rev. 127, 1248 (1962).

21. S. G. Thompson, Arkiv Fysik 36, 267 (1967).

22. J. R. Huizenga, R. Chaudhry, and R. Vandenbosch, Phys. Rev. 126, 210 (1962).

23. D. S. Burnett, R. C. Gatti, F. Plasil, P. B. Price, W. J. Swiatecki, and S. G. Thompson, Phys. Rev. 134, B952 (1964).

24. W. D. Myers and W. J. Swiatecki, Nucl. Phys. 81, 1 (1966).

25. S. Cohen and W. J. Swiatecki, Ann. Phys. (N.Y.) 22, 406 (1963).

26. K. J. LeCouteur and D. W. Land, Nucl. Phys. 13, 32 (1959).

27. C. Gustafson, I. L. Lamm, B. Nilsson, and S. G. Nilsson, Arkiv Fysik 36, 613 (1967).

28. V. M. Strutinski, Arkiv Fysik 36, 629 (1967).

29. W. Stepien and Z. Szymanski, Phys. Letters 26B, 181 (1968).

30. P. E. Nemirowsky and Yu. V. Adamchuk, Nucl. Phys. 39, 551 (1962).

APPENDIX

Angular Correction

The fission fragments coming at a given angle θ with respect to the beam axis constitute a cone which intercepts the cylindrical surface $\rho = R$ on which mica is present. When the mica is flattened out on a plane the equation of intercept will be: (See Fig. 12)

$$z^2 = R^2 \left(\frac{\cos^2 \frac{S}{R}}{\cos^2 \theta} - 1 \right) \tag{17}$$

where z, ρ and $\omega = \frac{S}{R}$ are the cylindrical coordinates.

When the mica scan is done in rectangular strips as shown in Fig. 12, one has to introduce a correction in the measured angular distribution due to the angular aberration. If the true angular distribution can be considered linear within the maximum and minimum θ values in the strip, the correction can be done exactly by substituting the nominal angle with the weighted average of the angle within the strip

$$\bar{\theta} = \frac{\int_{-z_{max}}^{+z_{max}} \int_{S_1}^{S_2} \theta(S,z)\,dS\,dz}{2 \cdot z_{max} \cdot (S_2 - S_1)} \tag{18}$$

The quantity $\theta(S,z)$ can be obtained from Eq. (17):

$$\theta(S,z) = \cos^{-1} \frac{\cos \frac{S}{R}}{\sqrt{1 + \frac{z^2}{R^2}}} \tag{19}$$

The double integral can then be evaluated numerically or the following approximation can be used:

for $\frac{z^2}{R^2} \ll 1$,

$$\theta(S,z) = \cos^{-1}\left[\left(1 - \frac{1}{2}\frac{z^2}{R^2}\right)\cos\frac{S}{R}\right] = \cos^{-1}\left[\cos\left(\frac{S}{R} + \delta\right)\right] \tag{20}$$

Expanding $\cos\left(\frac{S}{R} + \delta\right)$ to first order in δ and equalizing the expression to $\left(1 - \frac{1}{2}\frac{z^2}{R^2}\right)\cos\frac{S}{R}$, one obtains:

$$\delta = \frac{1}{2}\frac{z^2}{R^2} \cdot \frac{1}{\tan\frac{S}{R}} \quad . \tag{21}$$

Then Eq. (19) becomes:

$$\theta(S,z) = \frac{S}{R} + \frac{1}{2}\frac{z^2}{R^2} \cdot \frac{1}{\tan\frac{S}{R}} \tag{22}$$

With this approximate form, the double integral (18) can be evaluated in closed form and the result is

$$\overline{\theta} = \frac{S_2+S_1}{2R} + \frac{1}{6}\frac{z_{max}^2}{R(S_2-S_1)} \ln \frac{\sin\frac{S_2}{R}}{\sin\frac{S_1}{R}} \tag{23}$$

or

$$\overline{\theta} = \theta_{nom} + \frac{1}{6}\frac{z_{max}^2}{R(S_2-S_1)} \ln \frac{\sin\frac{S_2}{R}}{\sin\frac{S_1}{R}} \quad . \tag{24}$$

Since the expression (21) does not behave well near 0°, expression (24) cannot be used for very small angles, which in general are not accessible anyway. A comparison between the exact and the approximate expression is shown in Fig. 13.

Table I. K_o^2 versus excitation energy in ^{210}Po fission.

E_{lab} (MeV)	E_x (MeV)	K_o^2	Anisotropy W(180°)/W(90°)	$\langle \ell^2 \rangle$
29.0	23.0	3.31±0.68	6.05±0.54	89.723
30.0	24.0	8.85±0.58	3.73±0.13	99.400
31.0	25.0	13.14±0.63	3.16±0.08	109.154
31.5	25.5	15.86±0.66	2.92±0.07	114.052
32.0	26.0	14.91±1.29	3.09±0.14	118.960
32.5	26.5	17.61±0.56	2.88±0.05	123.877
33.0	27.0	18.40±0.71	2.87±0.06	128.801
33.5	27.4	20.11±0.79	2.79±0.06	133.731
34.0	27.9	20.60±0.64	2.81±0.05	138.664
34.5	28.4	23.96±0.72	2.63±0.04	143.601
35.0	28.9	24.47±1.27	2.65±0.07	148.539
35.5	29.4	28.67±1.00	2.48±0.04	153.480
36.0	29.9	28.41±1.24	2.53±0.06	158.420
36.5	30.4	29.54±0.72	2.52±0.03	163.361
37.0	30.9	29.79±1.30	2.55±0.06	168.302
37.5	31.4	31.17±0.60	2.52±0.02	173.242
38.0	31.9	28.94±1.46	2.67±0.07	178.180
38.5	32.4	31.43±0.63	2.59±0.03	183.117
39.0	32.8	33.57±1.26	2.53±0.05	188.052
40.0	33.8	36.13±1.75	2.50±0.06	197.916
41.0	34.8	34.47±0.81	2.63±0.03	207.769
42.6	36.4	38.05±1.48	2.59±0.05	223.510
45.0	38.7	42.96±1.47	2.56±0.04	247.058
50.0	43.6	48.72±1.41	2.63±0.04	295.853

Table II. K_o^2 versus excitation energy in ^{211}Po fission.

E_{lab} (MeV)	E_x (MeV)	K_o^2	Anisotropy W(180°)/W(90°)	$\langle \ell^2 \rangle$
31.0	22.8	13.57±0.51	3.11±0.06	109.796
32.0	23.8	16.39±0.56	2.94±0.05	119.637
32.5	24.3	17.69±0.55	2.88±0.05	124.571
33.0	24.8	17.91±0.89	2.92±0.08	129.512
33.5	25.3	21.83±0.66	2.68±0.04	134.458
34.0	25.8	22.97±0.70	2.65±0.04	139.408
34.5	26.2	22.35±0.87	2.74±0.06	144.362
35.0	26.8	24.53±0.86	2.66±0.05	149.317
35.5	27.2	25.63±1.16	2.64±0.06	154.274
36.0	27.7	25.05±0.88	2.72±0.05	159.232
36.5	28.2	28.77±0.97	2.56±0.04	164.189
37.0	28.7	29.59±1.12	2.56±0.05	169.146
37.5	29.2	31.91±1.34	2.50±0.05	174.103
38.0	29.7	34.64±1.36	2.43±0.05	179.058
39.0	30.7	38.88±1.50	2.35±0.05	188.963
40.0	31.6	37.74±1.34	2.45±0.04	198.859
41.0	32.6	37.66±1.25	2.52±0.04	208.746
42.0	33.6	41.28±1.48	2.45±0.04	218.620
43.0	34.6	42.33±1.24	2.48±0.04	228.483
44.0	35.6	44.14±1.46	2.48±0.04	238.332
46.0	37.5	52.43±1.93	2.36±0.04	257.988
48.0	39.5	56.64±2.79	2.35±0.06	277.586
50.0	41.5	60.88±3.04	2.34±0.06	297.125

FIGURE CAPTIONS

Fig. 1. Schematic drawing of the apparatus used in measuring angular distributions of fission fragments.

Fig. 2. Fission tracks in mica. Etching: 6 h. at room temperature in 48% hydrofluoric acid. The fission fragments have entered perpendicularly to the mica surface, therefore the picture shows the normal sections of the tracks. The large track is a pre-etched background track due to spontaneous fission of U^{238} in mica.

Fig. 3. Center of mass angular distribution of fission fragments in 29 MeV He^4 induced fission of Pb^{206}. The continuous line is the least-squares fit to the experimental data.

Fig. 4. Center of mass angular distribution of fission fragments in 50 MeV He^4 induced fission of Pb^{206}. The continuous line is the least-squares fit to the experimental data.

Fig. 5. Center of mass angular distribution of fission fragments in 31 MeV He^4 induced fission of Pb^{207}. The continuous line is the least-squares fit to the experimental data.

Fig. 6. Center of mass angular distribution of fission fragments in 42 MeV He^4 induced fission of Pb^{207}. The continuous line is the least-squares fit to the experimental data.

Fig. 7. K_o^2 dependence on excitation energy at the fission saddle point of Po^{210}. The arrow indicates the position of the fission barrier.

Fig. 8. K_o^2 dependence on excitation energy at the fission saddle point of Po^{211}. The arrow indicates the position of the fission barrier.

Fig. 9. Experimental values of K_o^2 in Po^{210} compared with the Fermi gas prediction (see text for the values of the parameters used).

Fig. 10. Schematic representation of the fission barrier of an even-even and odd-A nucleus in terms of a smooth single-particle model plus shell and pairing effects.

Fig. 11. Dependence of the gap parameter on the nuclear surface calculated using the assumption of Stepien and Szymanski.

Fig. 12. Drawing of a mica strip with lines of equal angle. The scanning is carried on in rectangular strips as indicated in the figure.

Fig. 13. Correction for the angular aberration introduced by the scanning technique. The two curves correspond to the exact and approximate expressions given in the text.

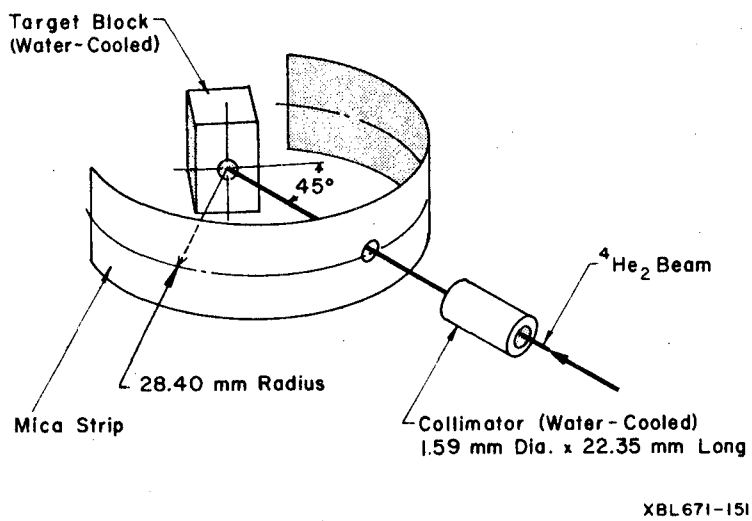
Target Block
(Water-Cooled)
45°
$^4He_2$ Beam
28.40 mm Radius
Mica Strip
Collimator (Water-Cooled)
1.59 mm Dia. x 22.35 mm Long
XBL671-151

Fig. 1

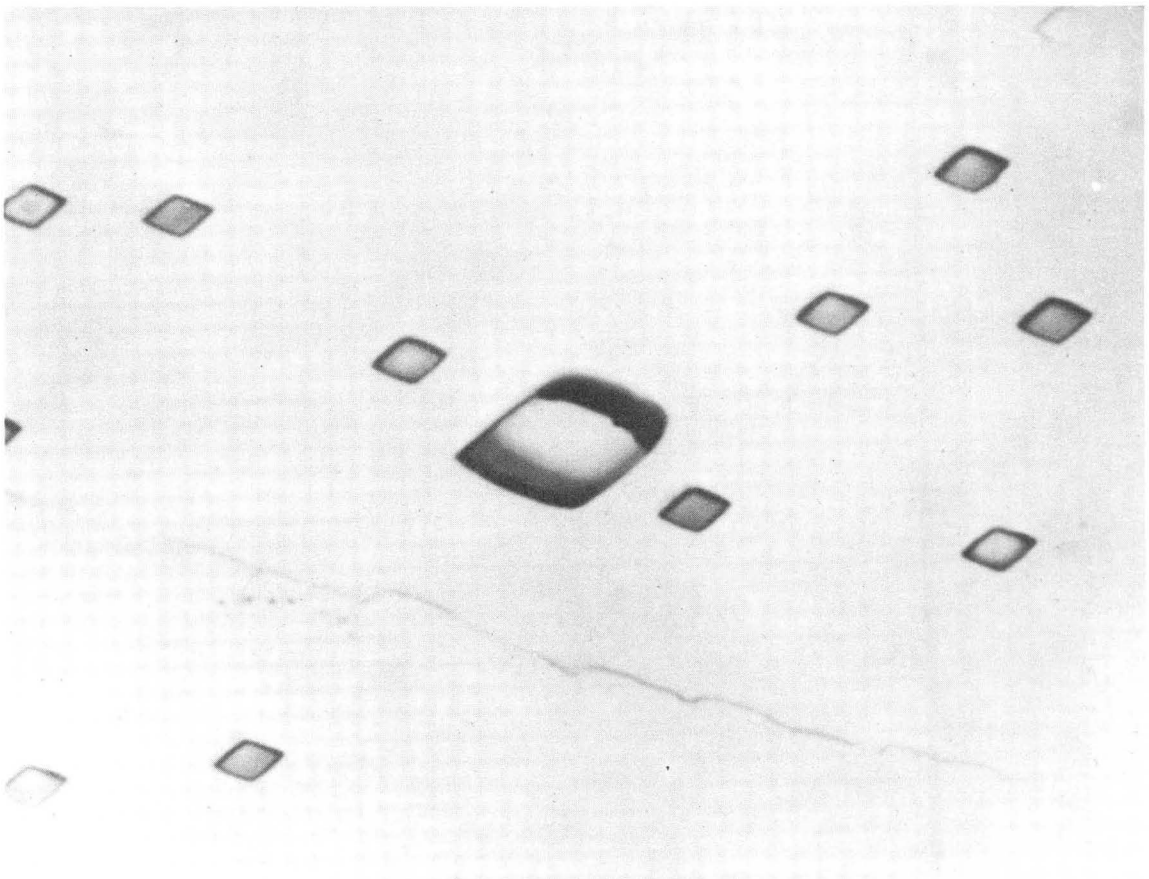

XBB 688-5113

Fig. 2

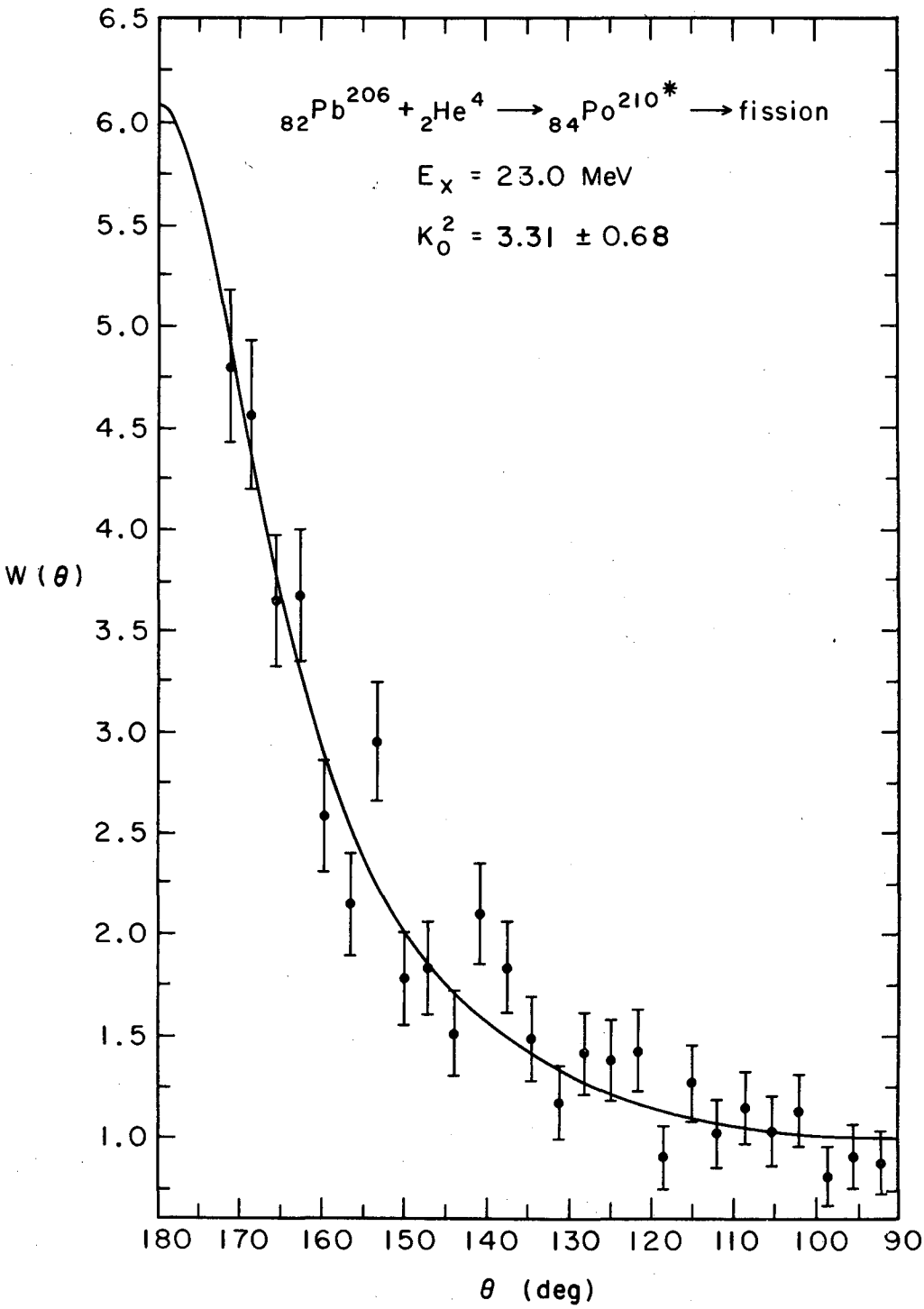

XBL686-2851

Fig. 3

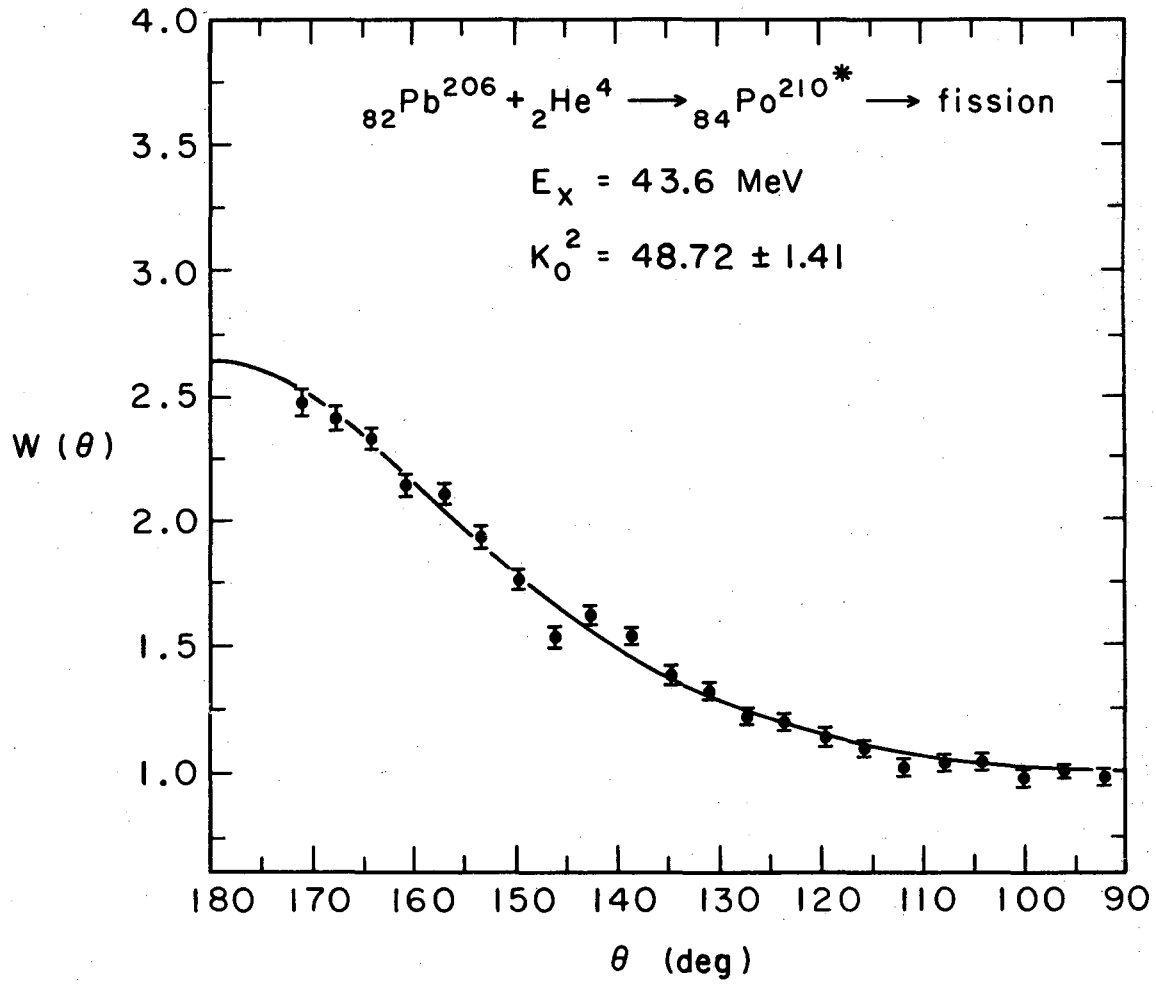

XBL686-2850

Fig. 4

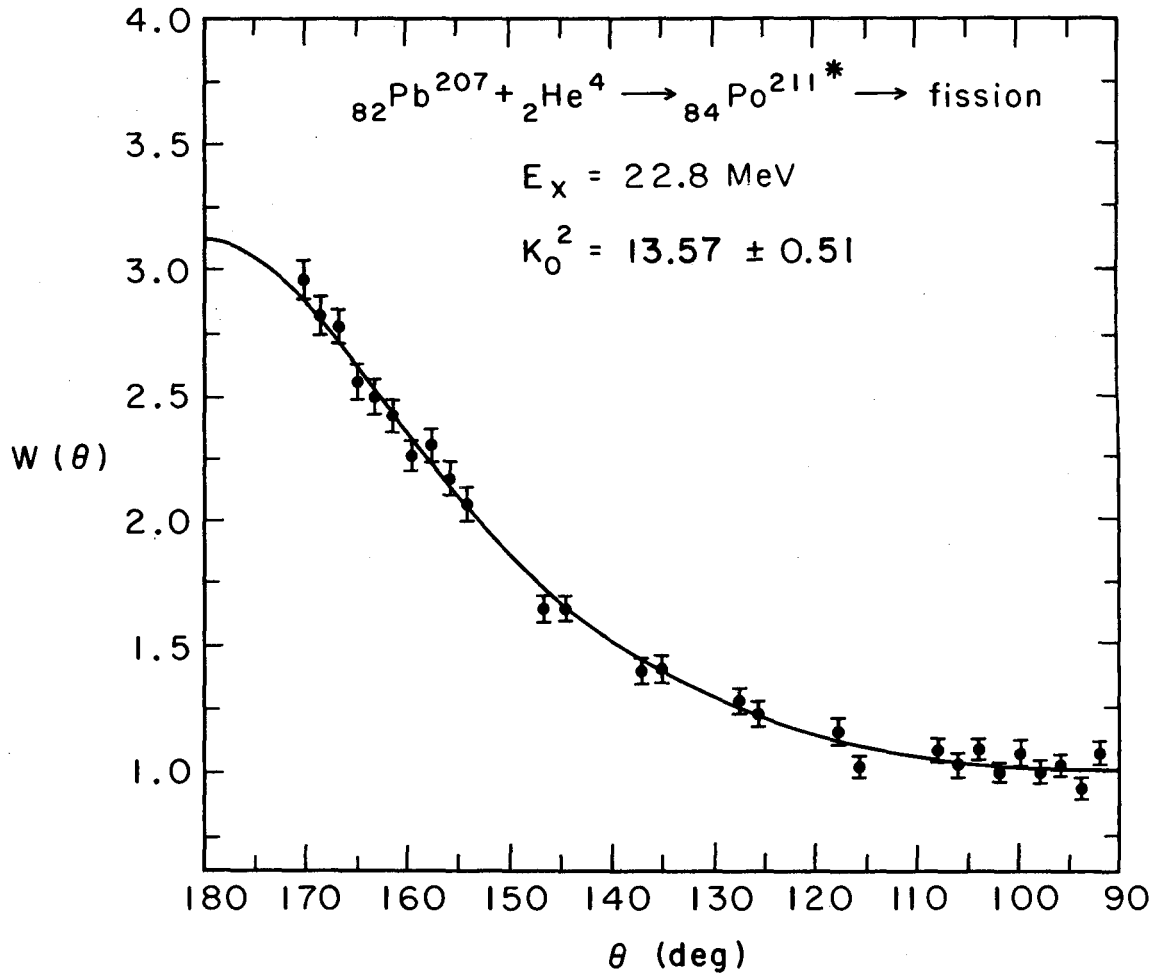

XBL686-2849

Fig. 5

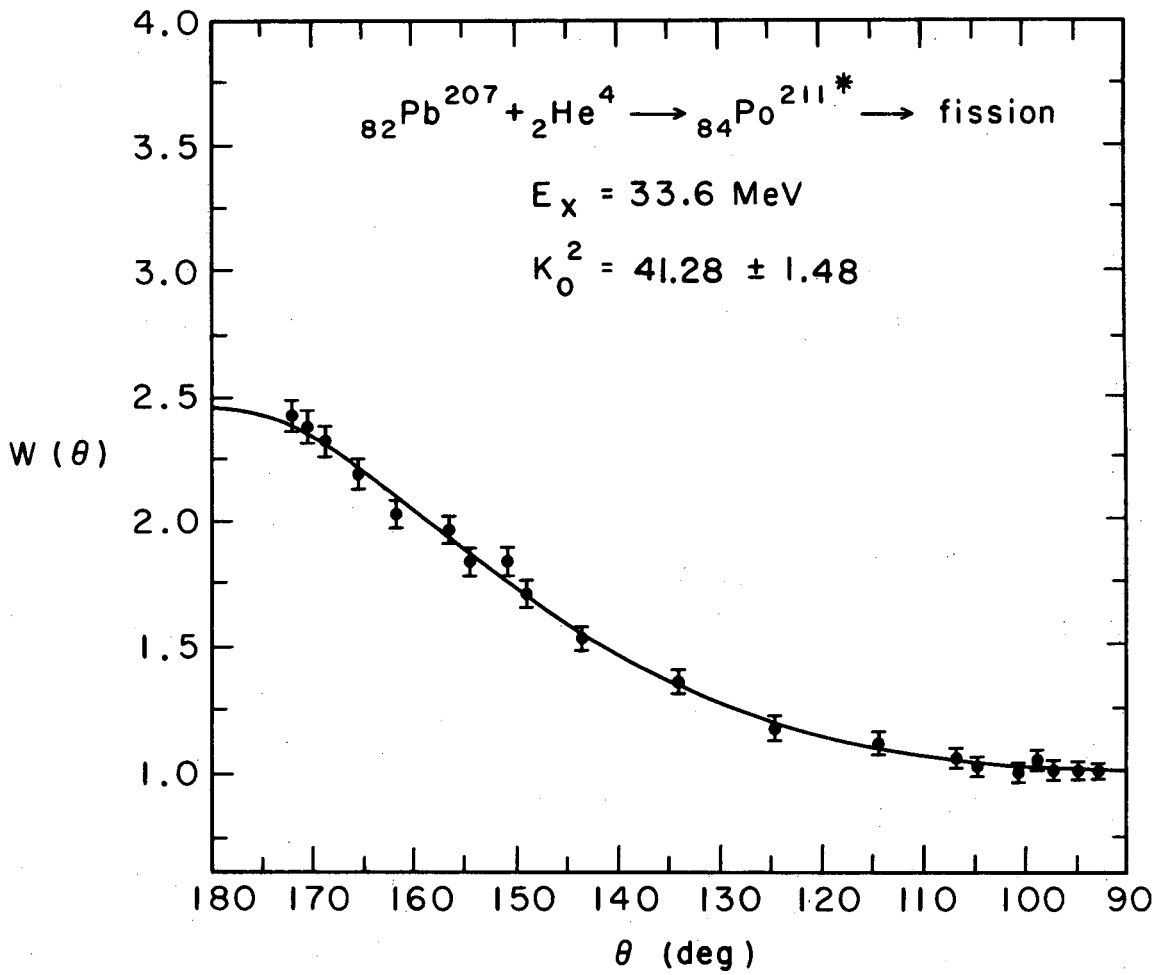

XBL686-2852

Fig. 6

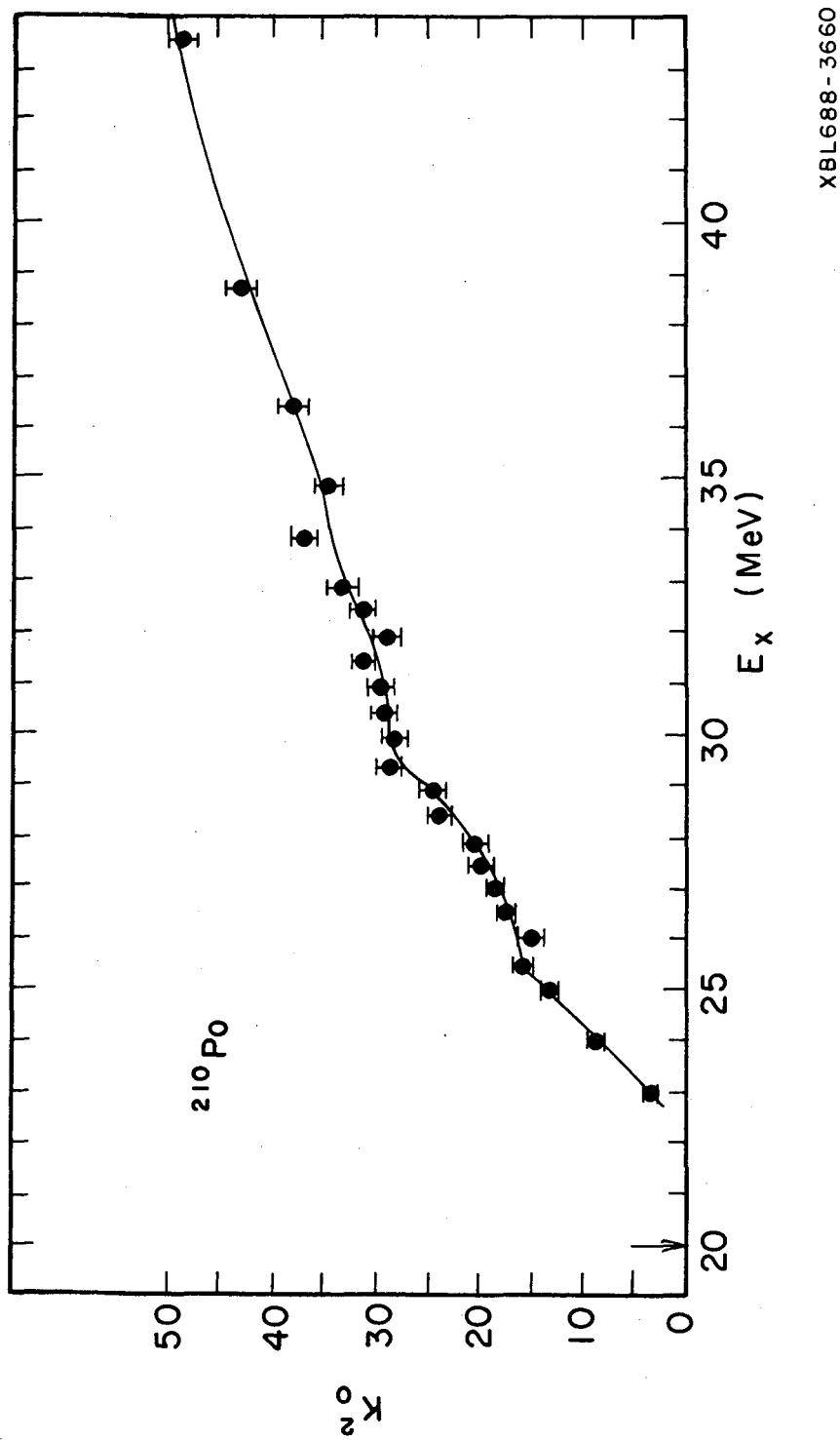

Fig. 7

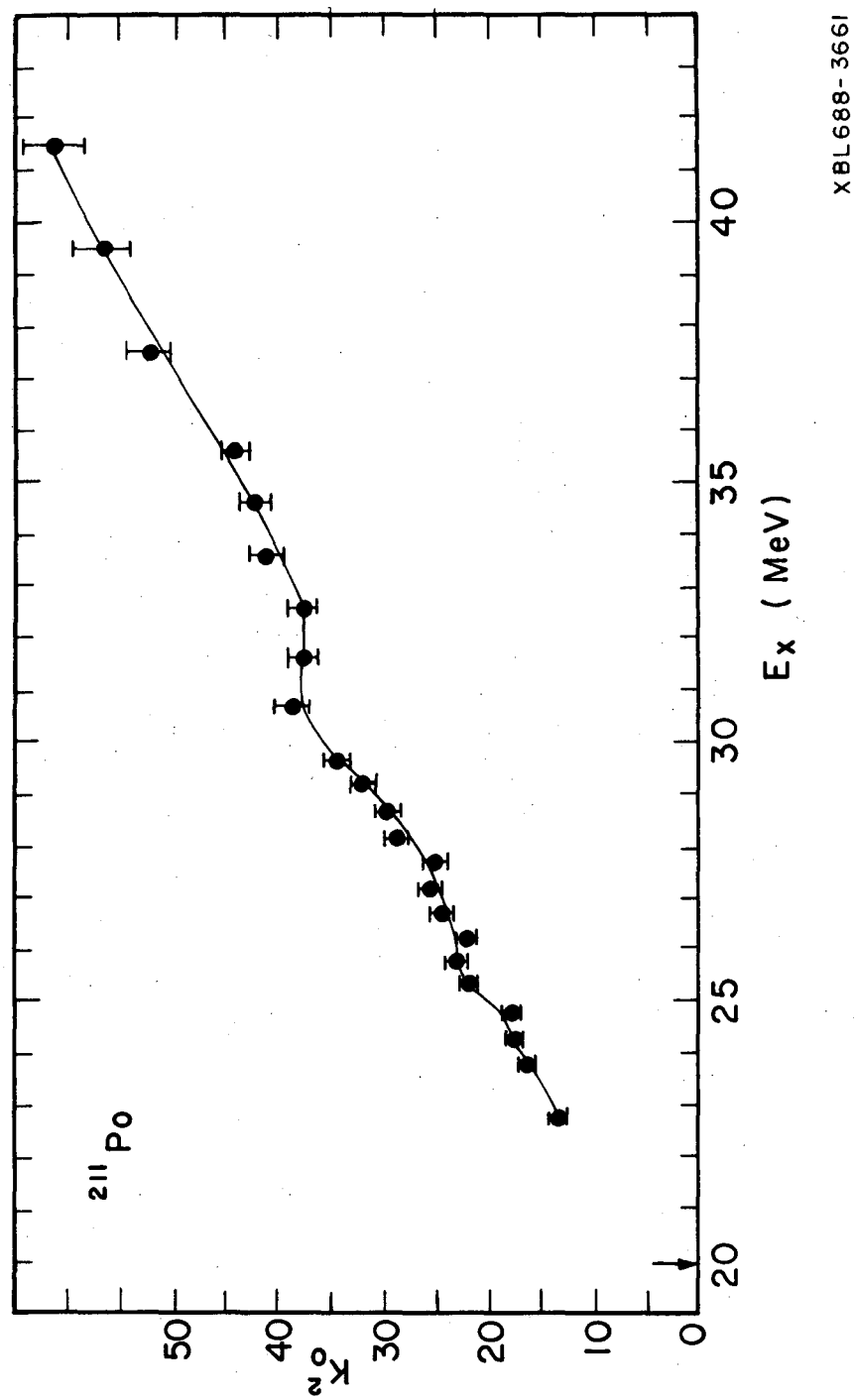

Fig. 8

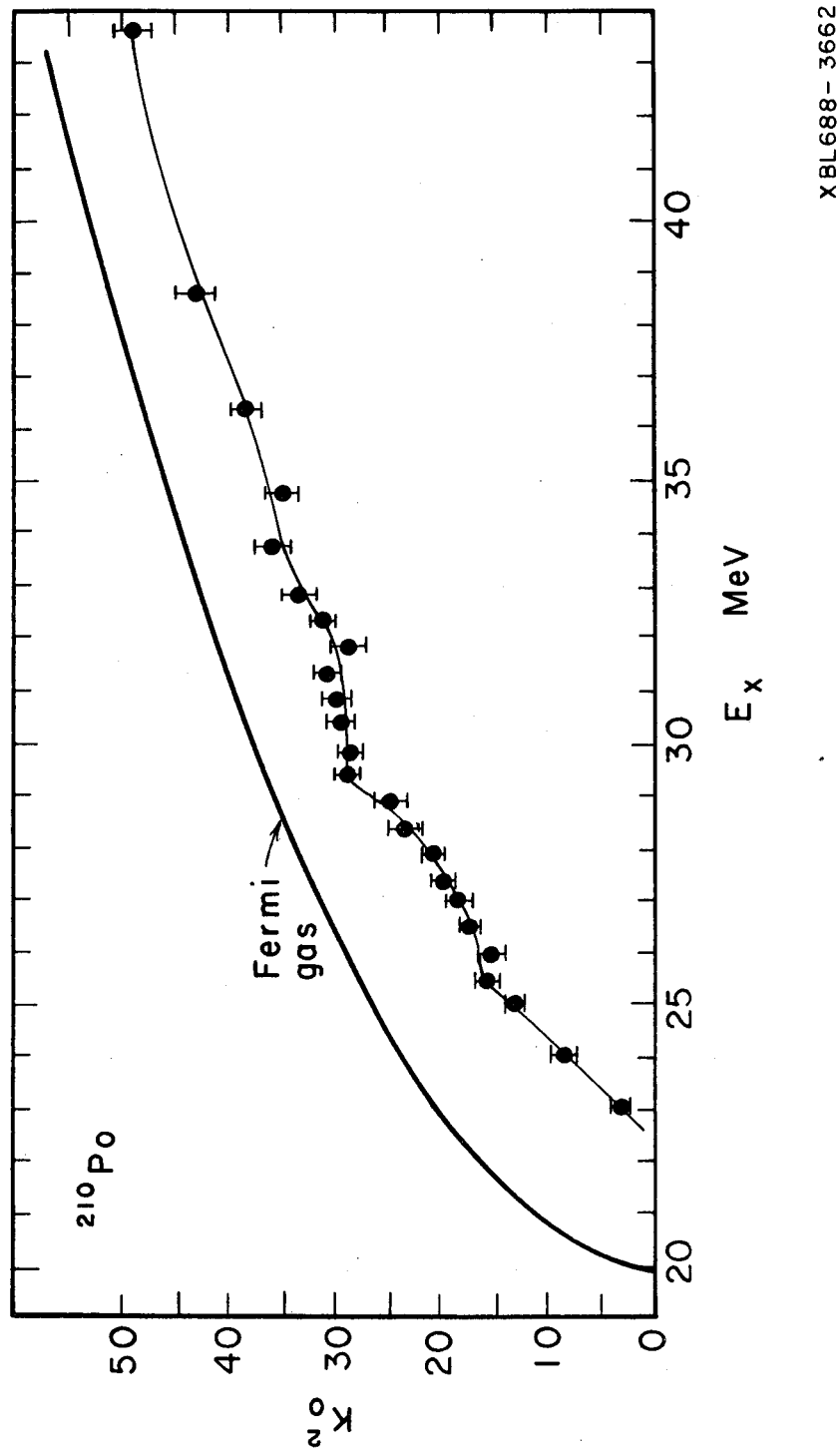
^{210}Po
Fermi gas
K_{o2}
0
10
20
30
40
50
20
25
30
35
40
E_x MeV
XBL688-3662

Fig. 9

Even - even

$$B_f^e = B_{sp}^e + \text{Shell}_g^e + C_g^e - \text{Shell}_s^e + - C_s^e$$

Odd - A

$$B_f^o = B_{sp}^o + \text{Shell}_g^o + C_g^o - \Delta g + - \text{Shell}_s^o - C_s^o + \Delta s$$

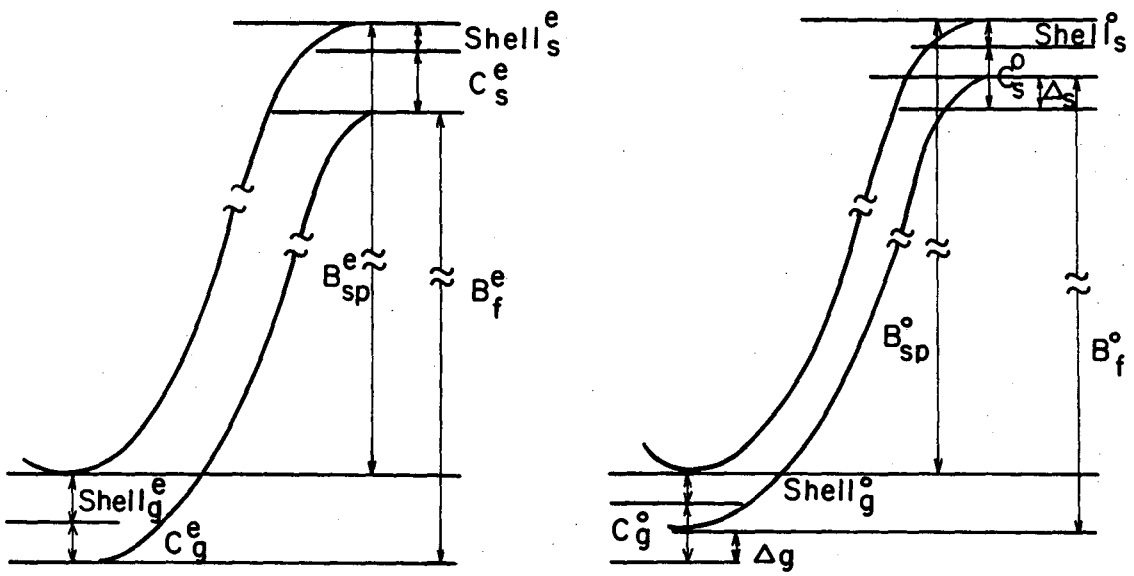

XBL688-3665

Fig. 10

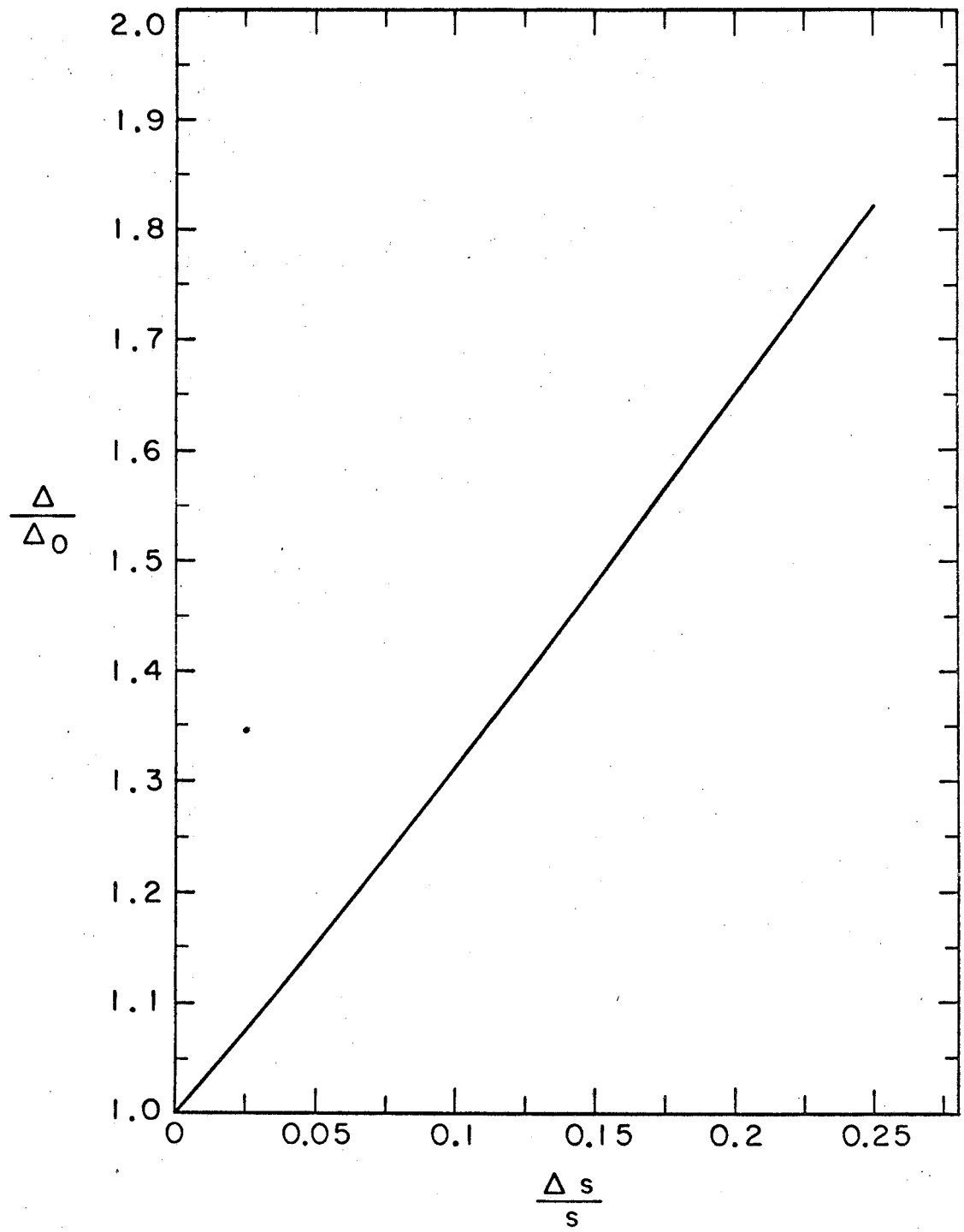

XBL686-2853

Fig. 11

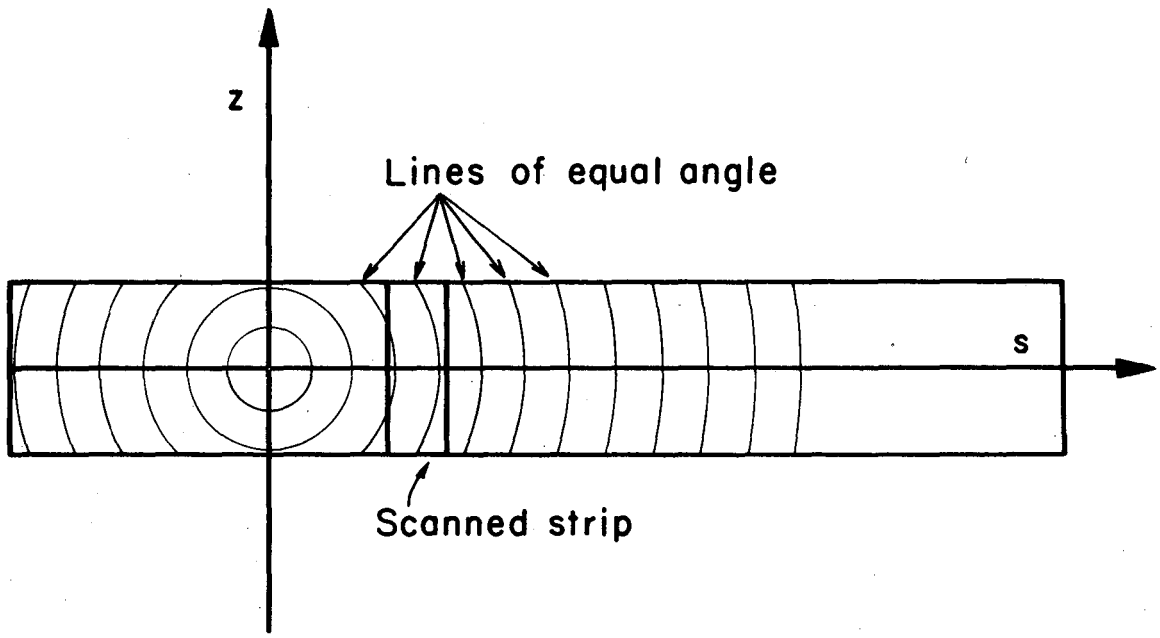

XBL688-3664

Fig. 12

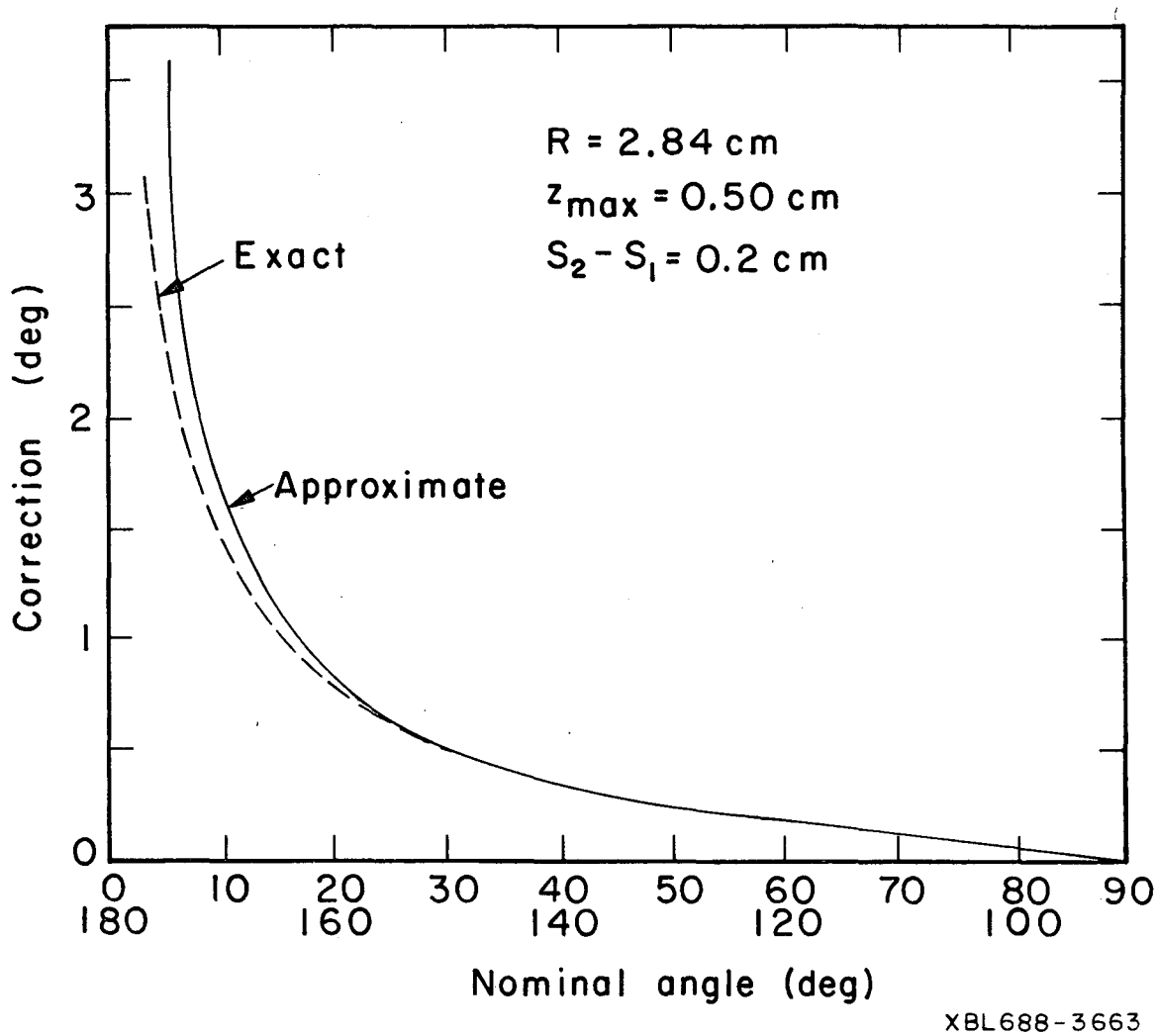
R = 2.84 cm
z_{max} = 0.50 cm
$S_2 - S_1$ = 0.2 cm
Exact
Approximate
Correction (deg)
0
1
2
3
0 10 20 30 40 50 60 70 80 90
180 160 140 120 100
Nominal angle (deg)
XBL688-3663

Fig. 13

This report was prepared as an account of Government sponsored work. Neither the United States, nor the Commission, nor any person acting on behalf of the Commission:

A. Makes any warranty or representation, expressed or implied, with respect to the accuracy, completeness, or usefulness of the information contained in this report, or that the use of any information, apparatus, method, or process disclosed in this report may not infringe privately owned rights; or

B. Assumes any liabilities with respect to the use of, or for damages resulting from the use of any information, apparatus, method, or process disclosed in this report.

As used in the above, "person acting on behalf of the Commission" includes any employee or contractor of the Commission, or employee of such contractor, to the extent that such employee or contractor of the Commission, or employee of such contractor prepares, disseminates, or provides access to, any information pursuant to his employment or contract with the Commission, or his employment with such contractor.